

# Evaluating Fluid Flow and Thermal Effects for Fuel Cell Humidity Sensor Design

Sven Reitz<sup>1</sup>, Andreas Wilde<sup>1</sup>, Jörg Bretschneider<sup>1</sup>, Karsten Sager<sup>2</sup>, Gottfried Richter<sup>2</sup>,  
Stefan Woschek<sup>2</sup>

<sup>1</sup>Fraunhofer Institute for Integrated Circuits, Division Design Automation, Dresden, Germany; <sup>2</sup>Intelligente Sensorensysteme Dresden GmbH, Dresden, Germany

[Received date; Accepted date] – to be inserted later

## Abstract

Modern fuel cells require high relative humidity (RH) of about 90% of the reactant gases hydrogen and oxygen/air in a temperature range of 70°C-90°C for optimum efficiency. Especially RH must be kept within tight tolerances, as condensed water would reduce effective area of the fuel cell electrodes, while lower humidity would dry out the fuel cell's membrane and lead to permanent damage. Humidity sensors should enable effective measurement and control of the reactants' relative humidity. However, under given harsh conditions, measuring RH poses several problems for standard, water adsorption based, polymer sensors. At high RH, measurements tend to be inaccurate and the polymer's permittivity properties tend to degrade. Furthermore, if the sensor is not well thermally isolated against the usually lower temperature of the environment, water will preferably condensate on the sensing element. Solutions to this problem require detailed modeling of heat transport by a pipe flow around a sensor socket embedded in a heat conductive and convective environment, evaluation of several constructive designs with respect to thermal sinks and inherent measurement errors. One approach investigated in this study was heating the sensor permanently, this way reducing RH and thus avoiding water condensation locally, but also introducing measurement errors which must be corrected. In this study, heat flow and humidity distribution around the sensor socket and at the sensors active area were analyzed using FE simulations coupled with additional equations for calculating RH in this harsh environment. These models allow investigating effective RH at the sensor element as function of parameters like inflow temperature, velocity and relative humidity, pipe wall temperature and sensor heating for several design variants of sensor placement in the flow as well as thermal isolation.

## 1. INTRODUCTION

Fuel cells with proton exchange membrane (PEMFC) are being studied intensively as a possible source of electrical energy to power vehicles, especially cars. In addition to the inherent advantages of this technique (use of renewable energies, no emissions, less loss of mechanical energy), efficiency plays a crucial role. To ensure optimal operation of a PEMFC, the process gases' – air and hydrogen – relative humidity must be as high as possible at operating temperature (70°C to 90°C), while avoiding condensation in any case.

Moisture of the usual process gases is steered in general by humidification. Due to already low (normal) process variations, occurring temperature changes at high humidity may lead very easily to condensation and thus can cause damage to the fuel cell. Thermodynamic laws of moist gas mixtures are the cause of this behavior, as e.g. described by the h-x or Mollier diagrams. At operating conditions close to the dew point (saturation, 100% relative humidity), even very small temperature changes can lead to qualitatively great changes of the gas mixture at critical points of the system. Low humidity on the membranes, on the one hand, will decrease electrical conductivity, causing increased Ohmic losses and, in extreme cases, the formation of holes in the membrane and therefore permanent damage to the fuel cell. At high humidity, on the other hand, possible flooding of the cathode may lead to a loss of fuel cell performance [1].

In fuel cells (in the automotive sector), process gases  $H_2$  and  $O_2$  are usually injected at high velocity to supply all cells simultaneously with process gas and thereby be able to get optimum voltage from the cell stack. The remaining gases which are emitted will be recycled, newly enriched with process gases, and humidified (see Fig. 1). Thus, it is possible to optimize process management in future fuel cell systems by controlling humidity.

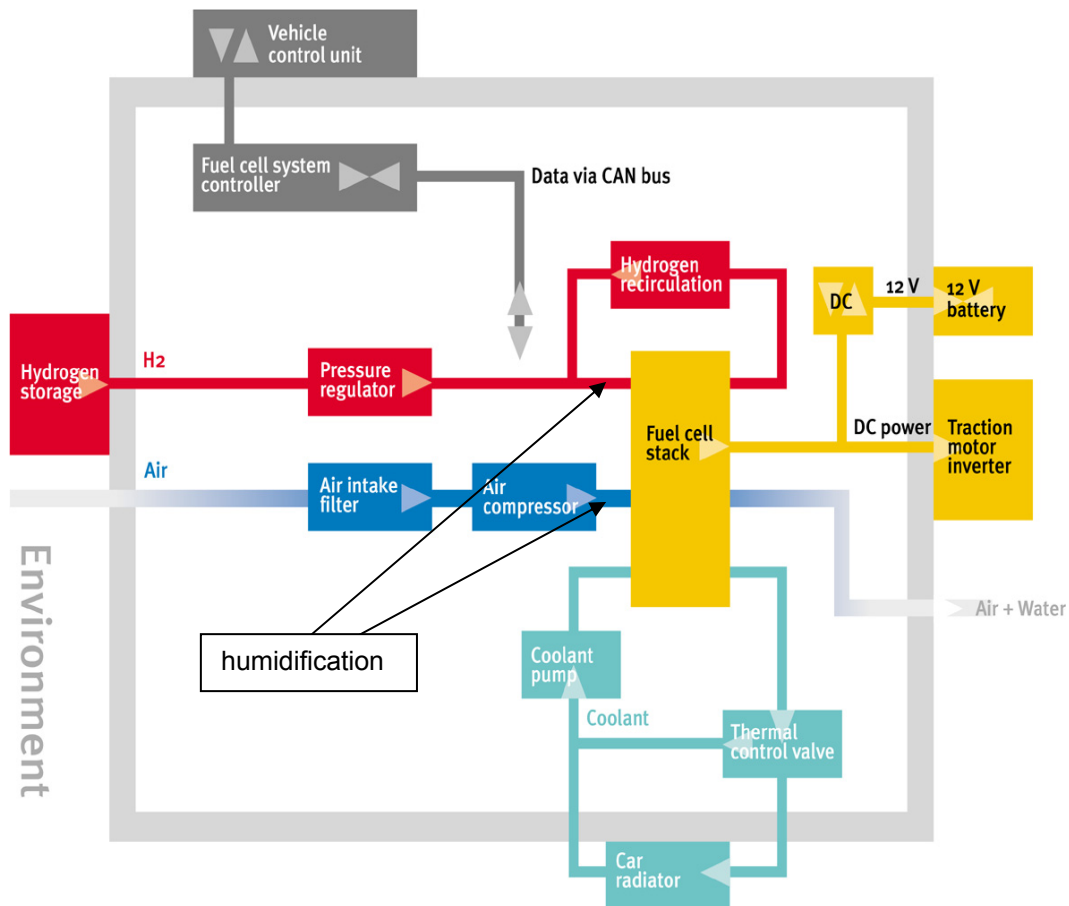


Figure 1. General Supply structure of a Proton Exchange Membrane Fuel Cell (PEMFC). Humidity is brought in both at the branch between the hydrogen recirculation port and the fuel cell stack and after air compression, requiring humidity sensors in place.

Critical in establishing optimized process control is precise measurement of relative humidity of the process gases at high temperatures with rather short response times [2]. While there are several methods to measure relative humidity of gases in principle, the dielectric method is particularly suitable for the application mentioned here. The dielectric method uses a polymer located between the electrodes of a capacitor, which can adsorb water from the gas, thus increasing its relative permeability and hence the capacity of the capacitor. However, due to physics and the metrological properties of the sensor, accuracy decreases with higher temperature and humidity. RH measurements at operating temperature and the required high relative humidity above 70% RH of a PEMFC will be too inaccurate. A possible strategy to reduce risk of damage and to achieve greater accuracy in the high-humidity range is heating the sensor element, thus lowering dew point and preventing condensation [3].

Long-term use of dielectric polymer sensors in highly humid environment (and also hydrogen) exhibits a drift of the sensor signal, caused by permanent adsorption of water into deeper pores of the polymer material, a process which is referred to as degradation in [4, 5, 6]. This drift can be eliminated to certain extent by overheating the sensor element more than  $100^{\circ}C$ . After annealing, it is then necessary to re-calibrate the sensor, before newly obtained measurements may be used.

By studying simulations, many complicated experimental setups and lengthy series of

measurements, e.g. for degradation analysis, can be omitted. Only selected measurements are necessary to calibrate simulation models appropriately. We will study, by appropriate modeling and simulation of the thermal and fluidic behavior of the humidity sensor system (Fig. 2), effects of heat sources integrated in the system at various places on temperature and RH of the process gas near the sensor element. Various constraints such as temperature, humidity, pressure and velocity of the fluid, heat exchange with the environment and heating power are to be considered. Variations in geometry and material of the sensor system will also be investigated in this contribution. The processes of degradation and subsequent healing-by-over-heating of the sensor system is left for further works.

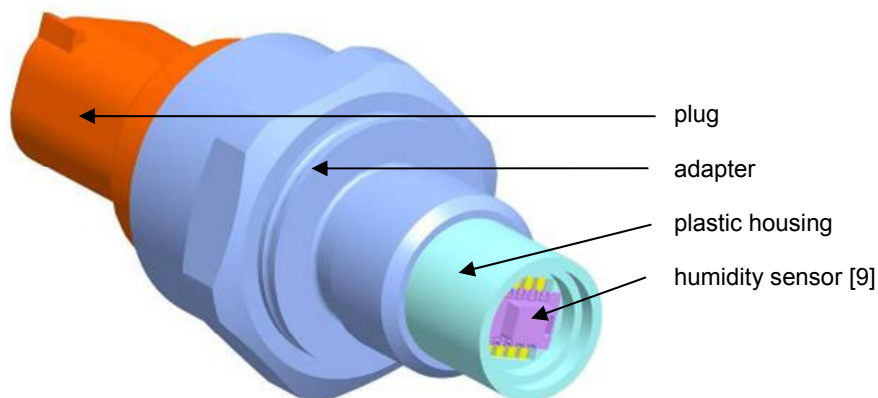


Figure 2. Humidity sensor system – variant 1

## 2. SIMULATIONS

### 2.1. Approach

For simulation of the humidity distribution in an environment of a dielectric polymer humidity sensor in the supply line of a fuel cell, an approach of gradual refinement– from simple to more complex models – and a stepwise modularization of simulation domains was chosen.

Due to quite geometric complex geometry, simulations of thermal and kinetic state variables of the process gases in an environment of the sensor were based on numerical finite element (FE) computation using ANSYS CFX [7]. We then fed results of the FE simulations into analytical thermodynamic models in order to determine relative humidity and dew point distribution.

Complexity of the simulation task stems from aspects of spatial resolution, dimension, geometry on its own, number and coupling of physical-technical quantities of interest, dynamic characteristics and the actual physical models of fluid flow and thermodynamics of the process gases. As any refinement of FE models is associated with increasing demands on computing power and memory, we applied appropriate model reduction methods such as symmetry, adaptive meshing and modularization as well as parallel simulation on a cluster computer.

Starting from vapor pressure models for humid air established in the domain of air conditioning and meteorology (Magnus formulae), we then went to evaluate models which are more suitable in the critical range of humidity, pressure and temperature in PEMFC applications.

Using an advanced miniaturized dielectric humidity sensor already on the market for standard applications, a key question was whether a heat source already integrated into the sensor IC would suffice to prevent condensation on the sensor element and to realize the desired drying cycles after degradation or if alternative system designs would have to be investigated [8]. According to the manufacturer's data sheet, the internal heat source was specified for calibration purposes only. Another issue was systematic measurement error introduced by permanently or occasionally heating the sensor element, which we wanted to describe more accurately in order to correct for it if necessary. We studied several constructive variants for this purpose.

Fig. 3 displays a CAD model of the sensor system, which had to be simplified in order to keep simulation times for variant computations within acceptable limits. In a first step, elements with very low thermal conductivity were dismissed (e.g. connector, internal circuit board, ...). The left part of the figure displays a more detailed view of the sensor adapter.

At the beginning, trends, feasibility, effects of environment and boundary conditions as well as transient analyses (response times) are in the focus of interest. Influence of model simplification will be considered later. Quasi-stationary flow simulations for the model in Fig. 3 ran ca. 12hs.

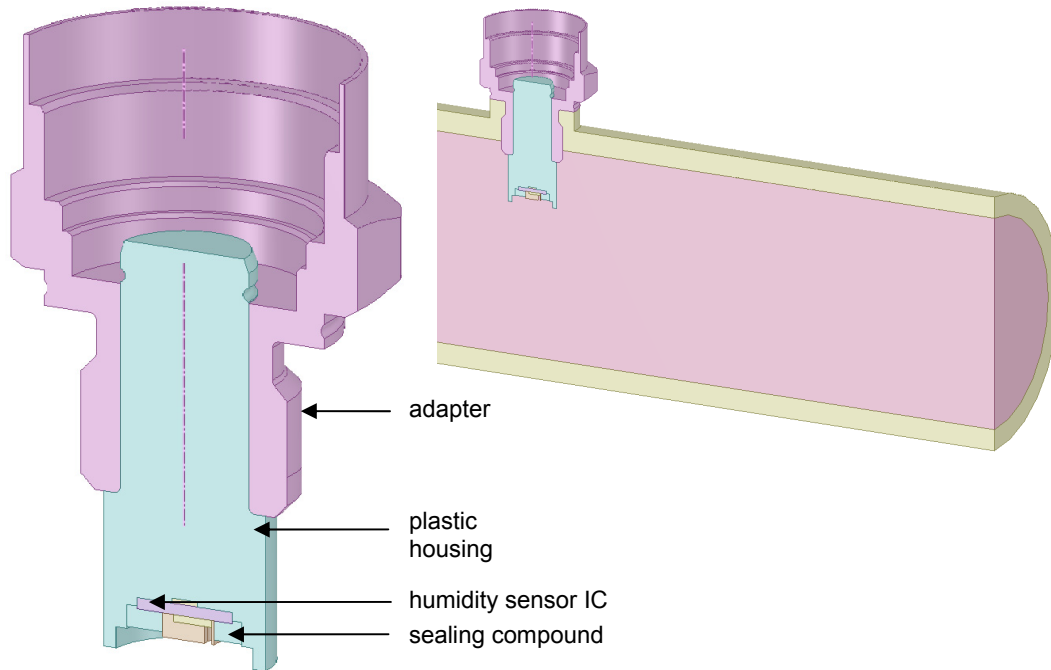


Figure 3. CAD model of the humidity sensor system with sensor IC, package, sealing compound, flange, pipe and flowing medium

## 2.2 Refined thermal model of the humidity sensor

For investigating the influence of the sensor IC's internal heater on relative humidity of the medium near the sensor element, the CAD model of the humidity sensor was refined by introducing thin CMOS layers for both the heating and the measuring element itself (Fig. 4). It was also necessary to know the exact location of the measuring element in order to export the correct data from ANSYS CFX to MATLAB for humidity calculations as described later. A third thin layer of copper conductor was also introduced to account for the thermal properties of the individual conductor lines upon the printed circuit board (epoxy).

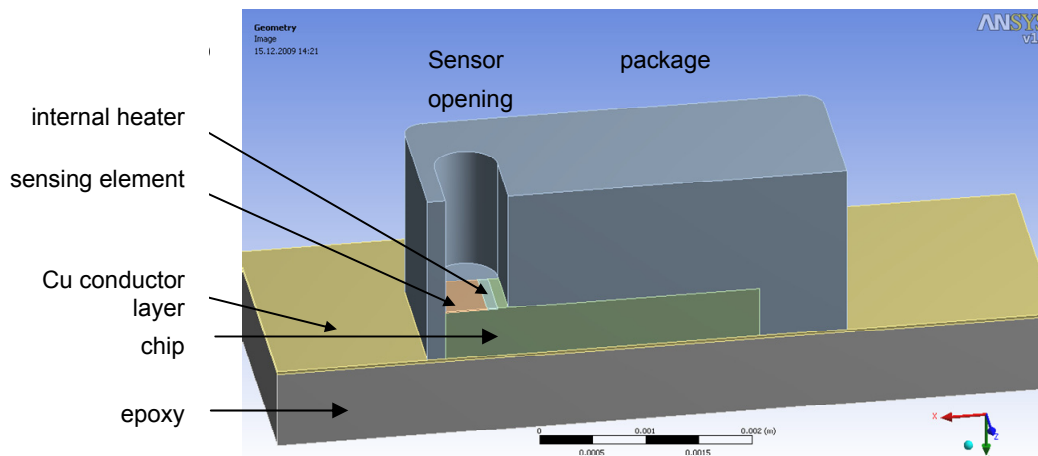


Figure 4. Refined thermal model of the humidity sensor [9] (sectional view)

Operating the integrated heating element with 8mA at 5V means a power dissipation of 40mW. To determine thermal inertia of the humidity sensor itself, a transient simulation over 200s with static air environment (zero velocity) was set up, switching heating power at  $t=1s$ . Extremal values of temperature within the measuring element are shown in Fig. 5. Obviously, the sensor is in thermal equilibrium after about 200s and the temperature difference across the measuring element is always less than  $0.18^{\circ}\text{C}$ . This relatively small difference allows assuming a homogeneous distribution of temperature and thus the measured RH within the measuring element itself.

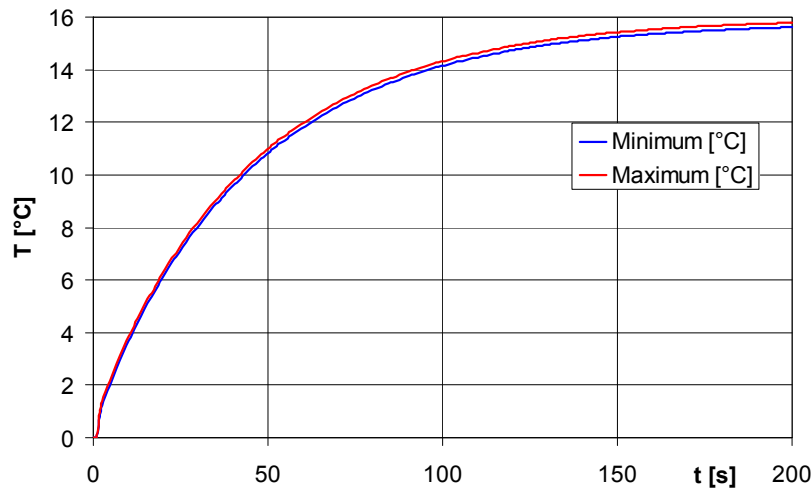


Figure 5. Heating of the sensing element over time, static medium

The resulting stationary final state of temperature of the humidity sensor is presented in Fig. 6, where the heater and the sensing element are the warmest spots and have been heated by about 16K, which fits well with corresponding measurements (see Fig. 15).

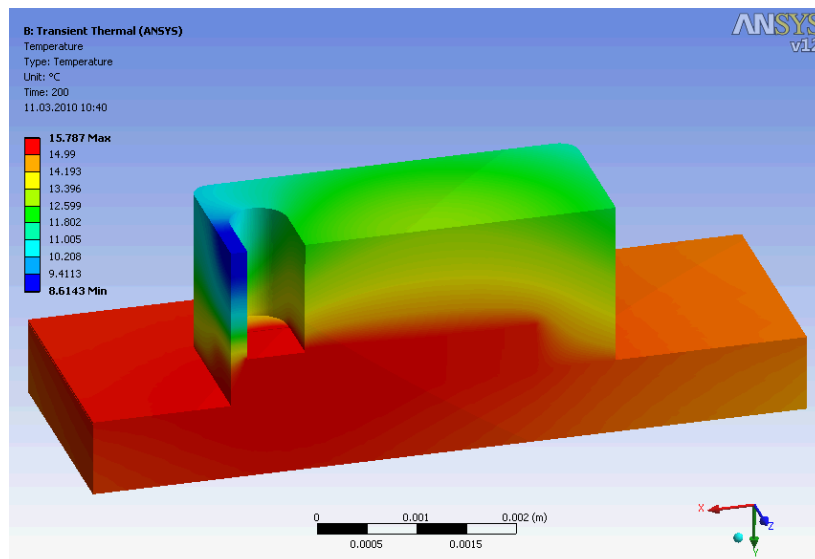


Figure 6. Heating of the humidity sensor due to internal heater

### 2.3. Integration of humidity equations in ANSYS CFX and MATLAB

The FE thermal flow simulation provided velocity, temperature, pressure & turbulence fields, but not yet relative humidity and dew point. As we wanted to evaluate several saturation vapor pressure models, we decided to separate FE and humidity simulations and to work just on an extract of nodes in the near environment of the sensor itself, thus dramatically reducing the number of nodes and thus computational efforts. As an exemplary model, we first implemented the saturation vapor pressure model usually referred to as Magnus' formulas, which are the

standard model in the air conditioning domain and also in meteorology. They are quite simple, but still sufficiently precise even in the temperature range of PEMFC to map general system behavior.

In ANSYS CFX it is possible to define own additional quantities or variables, and expressions using these quantities (see Figure 7).  $RH$  (relative humidity) is defined as the ratio between absolute water content  $x_{act}$  and saturation humidity  $x_{max}$ , capped at 100%. The total water content of the inflow medium is given by the PEMFC specification. In turn, saturation humidity  $x_{max}$  is a function of the saturation vapor pressure of water  $ED_{mag}$  in air, the specific gas constant for water vapor as well as temperature. Furthermore, a user variable  $myRH$  ("my" relative humidity) has been created with reference to expression  $RH$ . Since variable  $myRH$  is not based on differential equations, it must be calculated in the post processing step (result analysis), i.e. after flow simulation. The saturation vapor pressure in this example is calculated using the Magnus formula, which contains temperature dependencies again.

#### LIBRARY:

##### CEL:

##### EXPRESSIONS:

```
EDmag = 610.78*exp(17.08085*Temperature/(234.175+ Temperature))
```

```
Rwater = 8.314472/18.01528e-3
```

```
xmax = EDmag/Rwater/Temperature
```

```
xact = 207e-3
```

```
RH = min(xact/xmax*100,100)
```

```
END
```

```
END
```

```
END
```

Figure 7. Definition of RH as a user variable using Magnus' formula in ANSYS CFX

However, formulation of equations in CFX is somewhat complicated and there are other drawbacks. The coupled flow and temperature simulation and postprocessing can only be performed in the entire domain. As we were interested in the humidity and temperature values directly at and near the humidity sensor only, but with several variants for the vapor pressure model at saturation, we would spare a considerable amount of simulation time [10] in splitting up the simulation at this point.

We set up a modular simulation by exporting temperature data for selected subdomains of the ANSYS CFX geometry model, e.g. the sensor interfaces with the medium, to MATLAB, where the humidity field at these subdomains would be calculated according to various appropriated models, for comparison with experimental data. This drastic model reduction allows to "preprocess" the lengthy thermal flow simulations in batch mode and to swiftly and flexibly investigate the actual humidity values in MATLAB (Fig. 8). Re-import of these results in the CFX post-processing was done successfully. It turned out that, while Magnus was still a good approximation, the Goff-Gratch model was more accurate in the temperature range of PEMFC, while the similarly sophisticated Clausius-Clapeyron and Arden Buck models were dismissed.

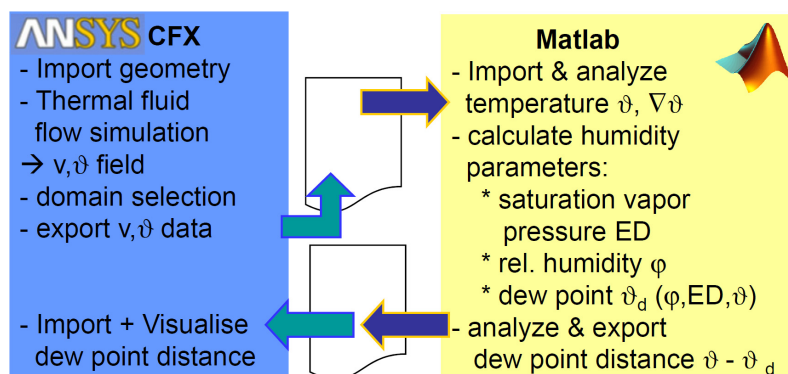


Figure 8. MATLAB-ANSYS modular simulation concept

## 2.4 Fluid flow simulation

Starting with the relatively simple, purely thermal model in Figure 4, we now move on to the more complex model of the real humidity sensor system in Figure 3 right. Foregoing details on individual material properties, boundary conditions used are specified here unless stated otherwise.

boundary	conditions
Inlet (from left)	air, $v = 40\text{m/s}$ , $\vartheta = 90^\circ\text{C}$ , $\text{rH} = 50\%$
Outlet (to right)	back pressure $p = 1\text{bar}$
Environment	static air, $\vartheta = 25^\circ\text{C}$ , convection coefficient $h=23\text{W/m}^2/\text{K}$
Power of internal heater	$P=40\text{mW}$

The quite complex geometry of the sensor system has major effects on the flow parameters, especially velocity, near the sensing element. Fig. 9 shows the velocity field for the boundary conditions in table 1. Before the plastic housing (flow is from left) the medium is retaining resulting in turbulences. At the edge of the housing, the medium is flowing about 40% faster than inflow, but a calm area is generated near the opening of the sensor element. This slowdown of the medium at the sensor “window” was intended by the construction of the nose in order to reduce dynamic load on the sensor.

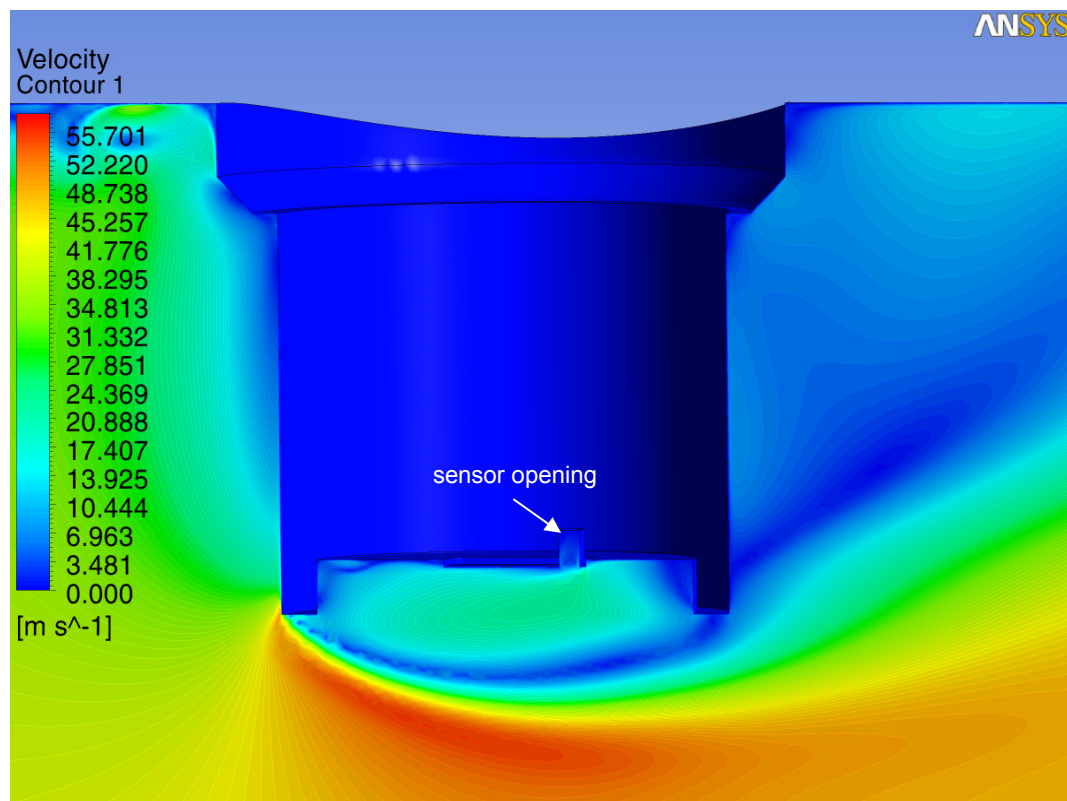


Figure 9. velocity field of the medium around the sensor housing

However, more interesting than medium velocity is the resulting temperature field both in the medium and the sensor system (especially at the sensing element).

Fig. 10 (left side) clearly shows the cooling down of the hot plastic housing from inflow medium temperature of 90°C (orange) down to 75°C (blue) at the pipe flange. On the other hand, at the opening of the humidity sensor, temperature of the medium is increased by 2.7K to 91.6°C (red, enlarged view in Fig. 10 right) due to the internal heater. Without heating, temperature was at only 88.9°C. Comparison with Figure 6 (15.8K warming without flow) exhibits the major effect of significant heat dissipation by both the rapidly flowing medium and the thermal conductivity of the pipe wall in connection with convection to the ambient, relatively cold air.

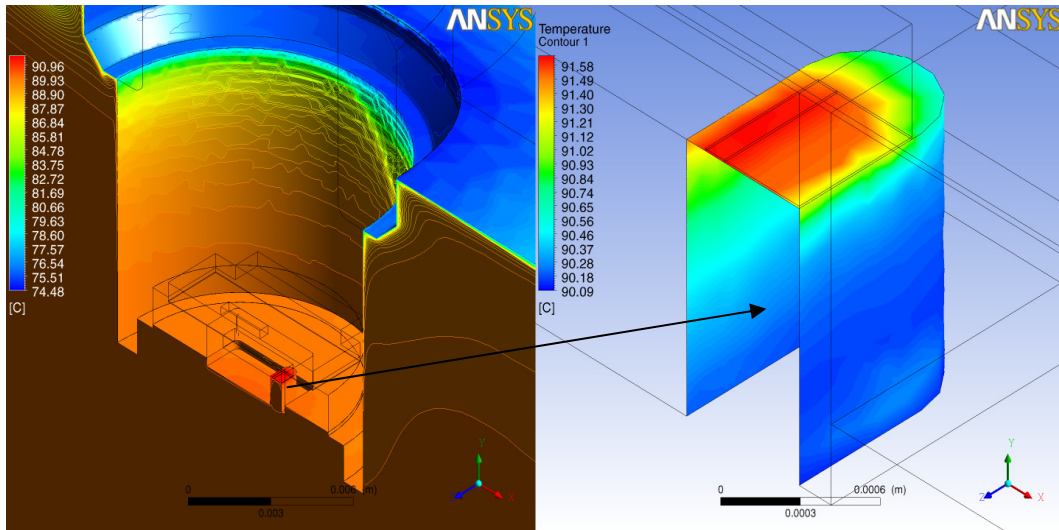


Figure 10. Media temperature with active internal heater - left: in the vicinity of the sensor; right: in the opening of the sensor package and on the humidity sensing element

Fig. 11 shows corresponding relative humidity of the medium, which decreases by about 2% due to the local heating from 50% of the incoming air to about 48% in the vicinity of the humidity sensor. In the unheated case, RH near the sensor is about 51.5% due to heat dissipation towards the environment (no figure). This indicates that heating power of the integrated heating element would be not enough in high-humidity conditions in order to avoid condensation on the sensor.

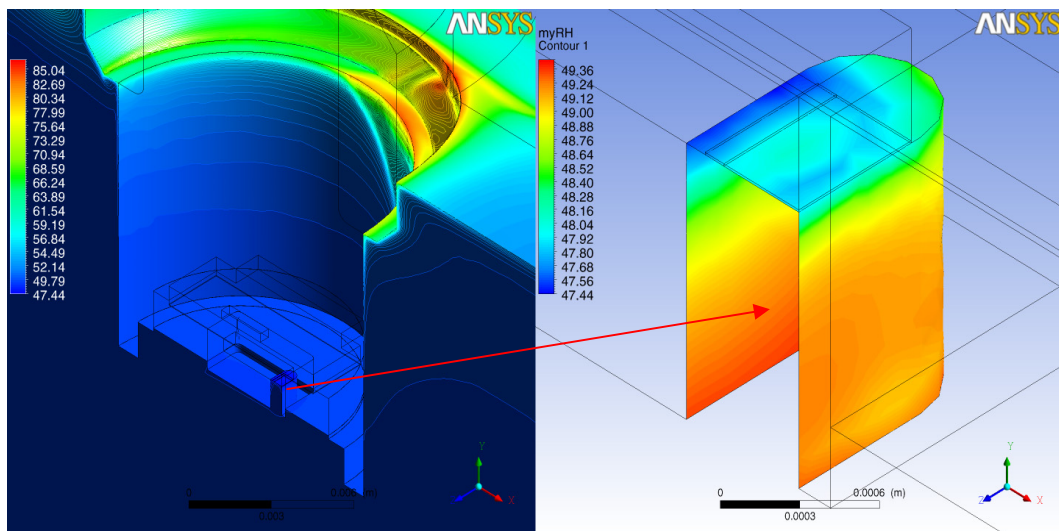


Figure 11. Relative humidity of the medium with internal heating, see Figure 10 for T



### 2.5. Alternative assembly variant of sensor system

In addition to the standard constructive version illustrated in Fig. 2 and 3, an alternative "pediculate" assembly variant was considered, where the humidity sensor is much more exposed to the medium, but also more "insulated" against the environment of the sensor system (Fig. 12). We were using the same simulation boundary conditions as in the standard design.

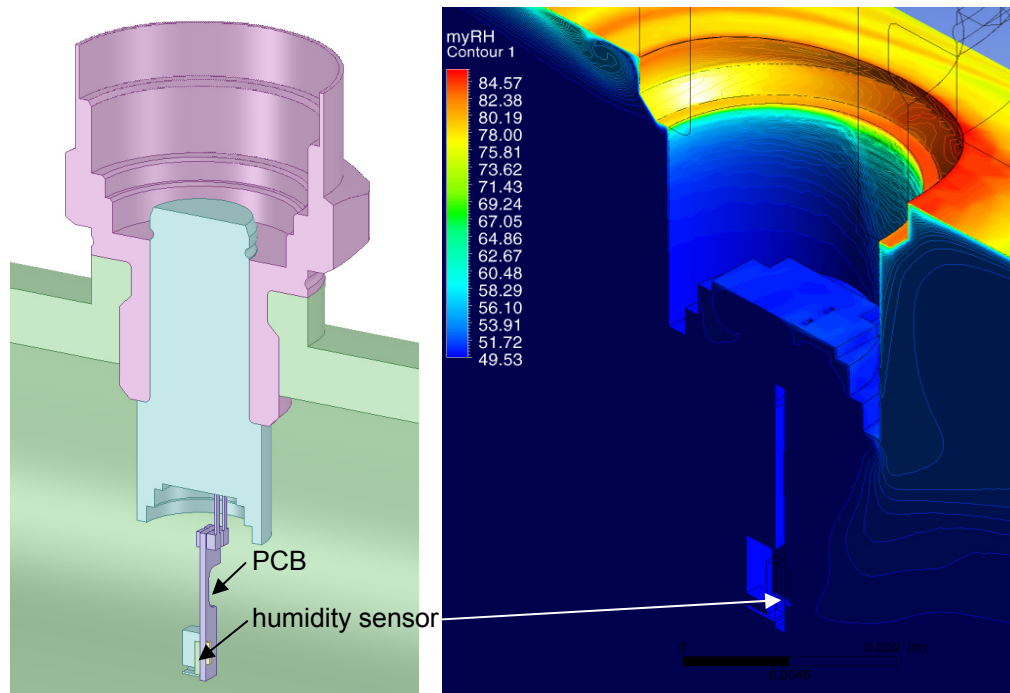


Figure 12. Left: alternative "pediculate" assembly variant; right: corresponding relative humidity distribution of the medium in the vicinity of the humidity sensor

Without internal heating, temperature and relative humidity distributions turn out to be significantly different for this variant. The fluid temperature at the humidity sensor decreases by only 0.03K, due to the considerably lower thermal conductivity towards the environment and the deep immersion of the sensor into the medium. These results have been confirmed by measurements. Accordingly, relative humidity increases by only 0.1%.

The right side of Fig. 12 exhibits the very homogeneous humidity distribution near the sensor. This desirable advantage of the "pediculate" variant faces the disadvantage of less protection of the humidity sensor against the fast flowing, hot and moist medium, which may shorten its reliability and life time. Nevertheless, this assembly variant is well suitable for reference measurements.

### 3. MEASUREMENTS

#### 3.1. Measurement test bench

At the heart of the humidity and temperature measurement test bench (Fig. 13) is a climate chamber which enables to drive any temperature and humidity testing regime. A very accurate reference sensor from Vaisala was placed beneath the test sensor assemblies into the climate chamber to be able to verify the accuracy of the measurement setup.

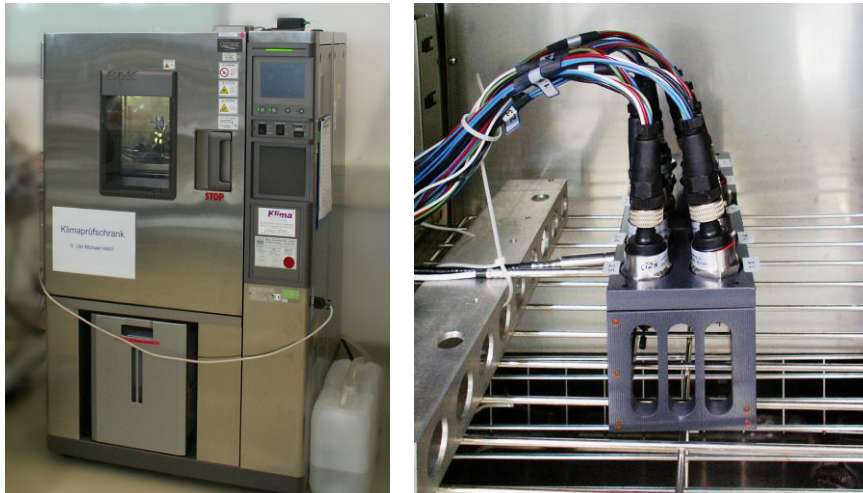


Figure 13. Measurement test bench Climate chamber and Sensor setup in the interior

For additional temperature reference measurements in the proximity of the sensor system, a NTC (negative temperature coefficient) resistor was attached to the sensor element (Fig. 14). All sensors including the reference sensor were arranged together as close as possible in the middle of the climate chamber in order to provide for nearly identical conditions.

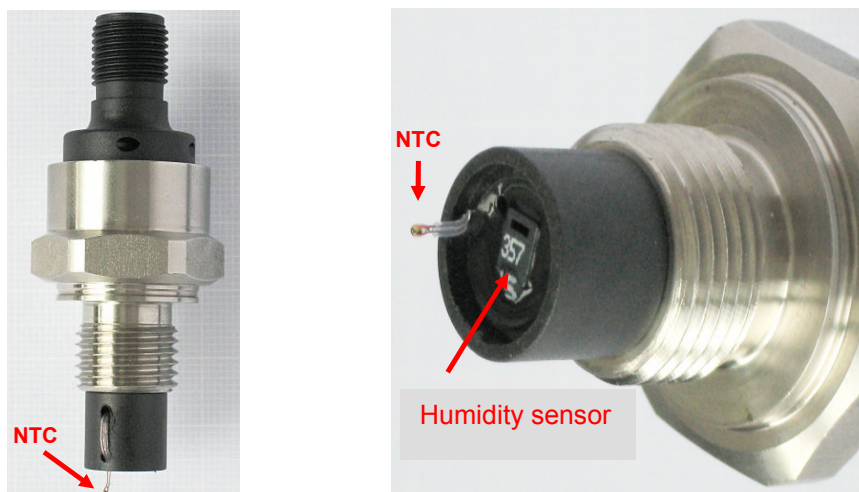


Figure 14. Humidity sensor system – assembly variant 1 with attached NTC element

The test bench captures the following quantities:

- Temperature dependant resistance value of the NTCs
- Readings of the sensors
- Measured values of the reference sensor

Furthermore, commands have to be sent to the sensors to switch internal heating on or off.

For automatic control of the test bench and data acquisition, a PC test program was developed which supplies up to 15 humidity sensors with a freely selectable temperature-humidity test

regime. Measurements are carried out periodically and the data are stored for later analysis. Using this hardware and software setup, complex and long-term measurement tasks can be automated.

### 3.2. First measurements on the test bench

To investigate settling characteristics of the sensors, series of measurements were carried out with static medium (zero velocity) and the internal heating was switched on and off at different period lengths. Fig. 15 shows exemplarily, that if heating endures, a steady state plateau of humidity and temperature values is achieved, after 300s in this case. When starting the heater, temperature increases at the measuring element and thus relative humidity is reduced. On switching off the heating, the process is reversed. The temperature gradient is approximately 16K, 99% of which is attained after half the steady state time, at 140s.

These results agree very well with the calculated temperature profiles of the refined humidity sensor model in Fig. 5 and confirm the thermal model.

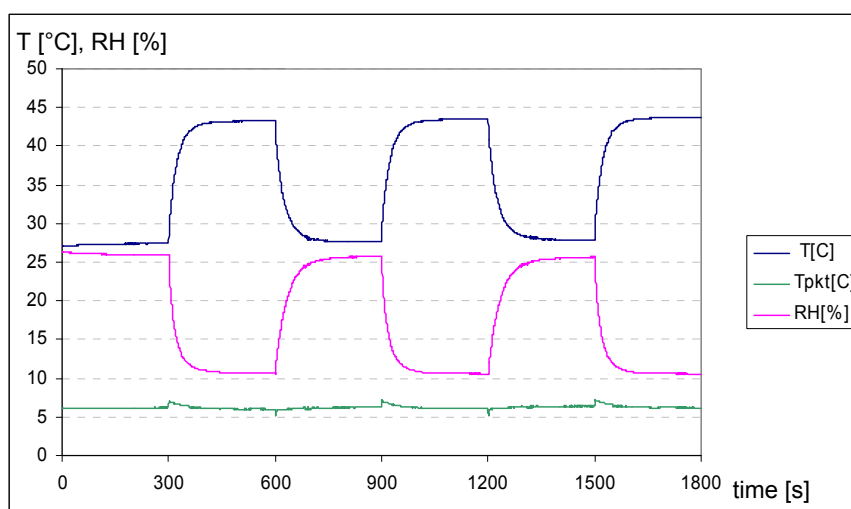


Figure 15. Transient behavior of temperature, relative humidity and dew point at the measuring element for 3 heating periods at room temperature

Further measurements with static medium were carried out in order to get general information on accuracy of the humidity sensors used for the tests, to check the test bench itself, and to record degradation data of the humidity sensors by first long-term runs. These data will then be used in corresponding simulation models and will replace costly measurements. The next step in measurements will be to switch to rapidly flowing media corresponding to the boundary conditions in real fuel cells. Using these new measurements, it will be possible to verify and evaluate the fluid flow simulations.

## 4. CONCLUSIONS

Thermal and fluid flow simulation models and results as well as measurement results for an integrated dielectric humidity sensor system for PEMFC systems have been presented. It was shown that heating can mitigate the crucial risk of condensation at the sensor elements and achieve higher accuracy in the high-humidity range, but that integrated heating elements of advanced sensors at the time would not have enough power to ensure safe operation of the humidity sensor and hence the fuel cell. Static medium simulations have been verified by first measurements. Further measurements with fast-flowing media will be carried out in the ongoing project.

## ACKNOWLEDGEMENTS

This paper is based on the project FEBREZ which is supported by the Sächsische Aufbaubank – Förderbank – under support-no. SAB 13547/2316. The authors of this paper are solely responsible for its content.

## REFERENCES

- [1] John P. Evans: *Experimental Evaluation of the Effect of Inlet Gas Humidification on Fuel Cell Performance*, Diplomarbeit Faculty of the Virginia Polytechnic and State University, 2003
- [2] R.H. Nishikawa, R. Kurihara , S. Sukemori , T. Sugawara , H. Kobayasi, S. Abe , T. Aoki, Y. Ogami, A. Matsunaga: *Measurements of humidity and current distribution in a PEFC*, Journal of Power Sources 155 (2006) 213-218
- [3] Vaisala Datenblatt „*How to measure Relative Humidity in Fuel Cells*“
- [4] Shanna D. Knights, Kevin M. Colbow, Jean St-Pierre, David P. Wilkinson: *Aging mechanisms and lifetime of PEFC and DMFC*, Journal of Power Sources 127 (2004) 127-134
- [5] J. St.-Pierre, D. P. Wilkinson, S. Knights and M. Bos: *Relationships between water management, contamination and lifetime degradation in PEFC*, Journal of New Materials for Electrochemical Systems, 3, 99-106 (2000)
- [6] Wietschel et. al., *Energietechnologien 2050 - Schwerpunkte für Forschung und Entwicklung, Technologienbericht/Politikbericht*, ISI-Schriftenreihe Innovationspotenziale, Hrsg.: Fraunhofer ISI, Fraunhofer Verlag, Stuttgart,2010, 1052 S./190S, S.50-55
- [7] ANSYS CFX documentation manuals
- [8] Schneider, P.; Eichler, U.; Einwich, K.; Schwarz, P.: *Simulation-based design of measurement systems*. "Sensor und Test", Nürnberg, 10.-12. Mai 2005
- [9] Sensirion AG: Datenblatt Feuchtesensor SHT1X
- [10] Schneider, P.; Reitz, S.; Bastian, J.; Schwarz, P.: *Combination of analytical models and order reduction methods for system level modeling of gyroscopes*. Nanotech 2005, MSM, Anaheim, California, 8.-12. Mai 2005